Excitation of K-shell electrons into ns states by the impact of charged particles

a V Nefiodov, G Plunien

Excitation of K-shell electrons into ns states by impact of charged particles

A.V. Nefiodov[1,2,*] and G. Plunien[3]

[1] *Petersburg Nuclear Physics Institute, 188300 Gatchina, St. Petersburg, Russia*
[2] *Max-Planck-Institut für Physik komplexer Systeme, D-01187 Dresden, Germany*
[3] *Institut für Theoretische Physik, Technische Universität Dresden, D-01062 Dresden, Germany*

(Dated: Received July 1, 2010)

We have investigated the excitation process of hydrogen-like multicharged ions by impact of different charged projectiles such as electrons, positrons, protons, and antiprotons. The universal scaling behaviour for the differential and total cross sections is deduced within the framework of the non-relativistic perturbation theory, taking into account the one-photon exchange diagrams. Special emphasis is laid on the description of the reaction in the near-threshold energy domain, which requires the accurate account for interactions between all particles in the colliding system.

(Some figures in this article are in colour only in the electronic version)

PACS numbers: 34.80.Dp

I. INTRODUCTION

Investigations of excitation processes of atomic targets by impact of charged particles are of fundamental importance. During last decades, the problem has been intensively investigated within the framework of different theoretical approaches (see, for example, the works [1–11] and references there). The deduction of the universal scaling behaviour of the differential and total cross sections is of particular interest, because it allows one to establish the most generic features of the excitation processes for a wide family of atomic systems. This problem can be solved within the framework of the non-relativistic perturbation theory, taking into account the one-photon exchange diagrams.

In the present paper, we shall consider the excitation of hydrogen-like multicharged ions by impact of different charged particles, such as electrons, positrons, protons, and antiprotons. The nuclear charge Z is supposed to be large enough ($Z \gg 1$), but it is assumed that $\alpha Z \ll 1$, where $\alpha \simeq 1/137.036$ is the fine-structure constant ($\hbar = 1$, $c = 1$). The parameter αZ gives the characteristic velocity of the bound K-shell electron. Since the atomic nucleus is much heavier than the projectiles, the former can be treated as a fixed source of the external field. Accordingly, to zeroth approximation, the particles are described by the Coulomb wavefunctions. The inter-particle interaction can be taken into account within the framework of the perturbation theory with respect to the correlation parameter $1/Z$. The accuracy of the theoretical calculations on the level of one-photon exchange diagrams is restricted by terms of the order of $1/Z$ and αZ. The relativistic corrections, which are of the order $\sim (\alpha Z)^2$, are neglected.

The stationary states of hydrogen-like atomic system are characterized by the principal quantum number n, the value of angular momentum l, and projection of the orbital angular momentum. The energy of the nl level is given by

$$E_{nl} = -\frac{I}{n^2} = -\frac{\eta_n^2}{2m}\,, \tag{1}$$

where $\eta_n = \eta/n$, $I = \eta^2/(2m)$ is the Coulomb potential for single ionization, $\eta = m\alpha Z$ is the average momentum of a K-shell electron, and m is the electron mass. In the following, we shall focus on excitation of the bound ns states only ($l = 0$).

II. ELECTRON IMPACT

Let us consider first the inelastic scattering of an electron. We shall derive formulas for differential and total cross sections of the excitation process $1s \to ns$ within the framework of the non-relativistic perturbation theory with respect to the electron-electron interaction. To leading order, the amplitude of the process under consideration is described by two Feynman diagrams depicted in Fig. 1. In the initial and final continuum states, the single-electron wavefunctions are denoted by ψ_p and ψ_{p_1},

*Corresponding author.
E-mail address: anef@thd.pnpi.spb.ru (A.V. Nefiodov).

respectively. The incident electron is characterized by the energy $E_p = \boldsymbol{p}^2/(2m)$ and the momentum $\boldsymbol{p}$ at infinitely large distances from the nucleus, while the scattered electron has the energy $E_{p_1} = \boldsymbol{p}_1^2/(2m)$ and the asymptotic momentum $\boldsymbol{p}_1$. The energy-conservation law implies $E_p + E_{1s} = E_{p_1} + E_{ns}$. In the momentum representation, the amplitude of the process reads

$$\mathcal{A} = \mathcal{A}_a\,\delta_{\tau_1'\tau_1}\delta_{\tau_2'\tau_2} - \mathcal{A}_b\,\delta_{\tau_2'\tau_1}\delta_{\tau_1'\tau_2}\,, \tag{2}$$

$$\mathcal{A}_a = \int \frac{d\boldsymbol{f}}{(2\pi)^3}\frac{d\boldsymbol{f}_1}{(2\pi)^3}\frac{d\boldsymbol{f}_2}{(2\pi)^3}\langle\psi_{p_1}|\boldsymbol{f}_1\rangle\langle\boldsymbol{f}_1+\boldsymbol{f}|\psi_p\rangle D(\boldsymbol{f})\langle\psi_{ns}|\boldsymbol{f}_2\rangle\langle\boldsymbol{f}_2-\boldsymbol{f}|\psi_{1s}\rangle\,, \tag{3}$$

$$\mathcal{A}_b = \int \frac{d\boldsymbol{f}}{(2\pi)^3}\frac{d\boldsymbol{f}_1}{(2\pi)^3}\frac{d\boldsymbol{f}_2}{(2\pi)^3}\langle\psi_{ns}|\boldsymbol{f}_1\rangle\langle\boldsymbol{f}_1+\boldsymbol{f}|\psi_p\rangle D(\boldsymbol{f})\langle\psi_{p_1}|\boldsymbol{f}_2\rangle\langle\boldsymbol{f}_2-\boldsymbol{f}|\psi_{1s}\rangle\,. \tag{4}$$

The quantities $\tau_{1,2}$ and $\tau_{1,2}'$ denote the spin projections of the Pauli spinors in the initial and final states, respectively. The photon propagator $D(\boldsymbol{f}) = 4\pi\alpha/f^2$ describes the instantaneous exchange by a Coulomb photon with the momentum $\boldsymbol{f}$. The amplitude $\mathcal{A}_a$ corresponds to the direct diagram, while the amplitude $\mathcal{A}_b$ is due to the exchange diagram. The latter results due to the identity of electrons.

Let us focus first on the asymptotic non-relativistic energies E_p within the range $I(1-n^{-2}) \ll E_p \ll m$. In this case, $E_{p_1} \sim E_p$ and the asymptotic momentum of the scattered electron is estimated as $p_1 \sim p \gg \eta$. Accordingly, one needs to take into account only the Feynman diagram depicted in Fig. $1(a)$. The contribution of the exchange diagram turns out to be significantly suppressed and, therefore, can be neglected. The wavefunctions of the incident and scattered electrons can be approximated by the plane waves (Born approximation):

$$\langle\boldsymbol{f}_1+\boldsymbol{f}|\psi_p\rangle \simeq \langle\boldsymbol{f}_1+\boldsymbol{f}|\boldsymbol{p}\rangle = (2\pi)^3\delta(\boldsymbol{p}-\boldsymbol{f}-\boldsymbol{f}_1)\,, \tag{5}$$

$$\langle\psi_{p_1}|\boldsymbol{f}_1\rangle \simeq \langle\boldsymbol{p}_1|\boldsymbol{f}_1\rangle = (2\pi)^3\delta(\boldsymbol{p}_1-\boldsymbol{f}_1)\,. \tag{6}$$

Then the amplitude (3) is simplified and can be cast into the following analytic form [12]

$$\mathcal{A}_a = 4\pi\alpha\,\eta^{-5}N_1N_nT_n(x)\,, \tag{7}$$

$$T_n(x) = \frac{2\pi}{ix^3}\left\{\frac{(ix-\tau_-)^{n-1}}{(ix-\tau_+)^{n+1}} - \frac{(ix+\tau_-)^{n-1}}{(ix+\tau_+)^{n+1}}\right\}, \tag{8}$$

where $x = q/\eta$, $\tau_\pm = 1 \pm n^{-1}$, $N_n^2 = \eta_n^3/\pi$, $\eta_1 = \eta = m\alpha Z$, and $\boldsymbol{q} = \boldsymbol{p} - \boldsymbol{p}_1$ is the momentum transfer. Although the dimensionless function (8) is written in the complex form, it is a real function depending actually on x^2.

The total cross section for the excitation process is given by [12]

$$\sigma_{ns}^* = \frac{\sigma_0}{Z^4}\,Q_n(\varepsilon)\,, \quad (n \geqslant 2)\,, \tag{9}$$

$$Q_n(\varepsilon) = \frac{\varkappa_n}{n^3\varepsilon}\,, \tag{10}$$

$$\varkappa_n = \frac{8}{\pi^2}\int\limits_0^\infty dx\,x\,T_n^2(x) \tag{11}$$

$$= \frac{2^6}{(2n+1)!}\frac{d^{2n+1}}{dx^{2n+1}}\left[\frac{\ln x}{x^5}(x-i\tau_-)^{2n-2}\right]_{\big|\,x=i\tau_+} - \frac{2^7}{n!}\frac{d^n}{dx^n}\left[\frac{\ln x}{x^5}\frac{(x^2+\tau_-^2)^{n-1}}{(x+i\tau_+)^{n+1}}\right]_{\big|\,x=i\tau_+}, \tag{12}$$

where $\sigma_0 = \pi a_0^2 \simeq 87.974$ Mb and $a_0 = 1/(m\alpha)$ is the Bohr radius. Here we have introduced the dimensionless energy of the incident electron $\varepsilon = E_p/I$, which is related with the dimensionless energy of the scattered electron $\varepsilon_1 = E_{p_1}/I$ and the threshold energy of the process $\varepsilon_{\text{th}} = 1 - n^{-2}$ as follows $\varepsilon = \varepsilon_1 + \varepsilon_{\text{th}}$. In Eq. (12), the regular branch of the logarithm is chosen, which assumes real values on the upper edge of the cut made along the positive semi-axis. After taking the derivatives with respect to x, one should set $x = i\tau_+$. The function $Q_n(\varepsilon)$ does not depend on the nuclear charge Z, that is, it is universal. The numerical coefficients $\varkappa_n$ are presented for few values of the principal quantum numbers n in Table I. The formulas (9)–(12) are justified in the asymptotic high-energy domain characterized by $1 \ll \varepsilon \ll 2(\alpha Z)^{-2}$. It is easy to see that the integral in Eq. (11) is saturated within the range $0 \leqslant x \lesssim 1$. This means that in the process of excitation of the K-shell electron by fast projectiles the characteristic momentum transfer q is of the order of η.

In the limit $n \to \infty$, Eqs. (8) and (11) take the form

$$T_\infty(x) = 4\pi y^2x^{-3}e^{-2y}\Big\{2x\cos(2xy) + (x^2-1)\sin(2xy)\Big\}\,, \quad y = (1+x^2)^{-1}\,, \tag{13}$$

$$\varkappa_\infty = 2e^{-4}\Big\{16\Big[\text{Ei}(4) - \gamma_{\text{E}} - \ln 4\Big] - 179 - e^4\Big\} \simeq 1.798\,. \tag{14}$$

Here $\mathrm{Ei}(z)$ is the exponential integral function, $\gamma_{\mathrm{E}} \simeq 0.5772$ is the Euler's constant, and $e \simeq 2.71828$.

In the near-threshold energy domain characterized by $I(1-n^{-2}) \lesssim E_p$, the theoretical description of the problem becomes more complicated, because it requires an accurate account for both the electron-electron and electron-nucleus interactions. In this case, $E_{p_1} \sim E_p \sim I$ and the asymptotic momenta of the incident and scattered electrons are estimated as $p_1 \sim p \sim \eta$. The direct and exchange amplitudes give rise to comparable contributions to the cross section.

In the following, we shall evaluate the amplitudes (3) and (4) without further simplifications. The Coulomb wavefunctions for bound states are given by the integral representations

$$\langle \boldsymbol{f}_2 - \boldsymbol{f}|\psi_{1s}\rangle = N_1\Big(-\frac{\partial}{\partial\eta}\Big)\langle \boldsymbol{f}_2|V_{i\eta}|\boldsymbol{f}\rangle\,, \tag{15}$$

$$\langle \boldsymbol{f}|\psi_{ns}\rangle = \frac{N_n}{2\eta}\oint\limits_{(\eta_n^+)}\frac{dy}{2\pi i}\frac{(y+\eta_n)^n}{(y-\eta_n)^n}\Big(-\frac{\partial}{\partial\lambda}\Big)\langle \boldsymbol{f}|V_{i\lambda}|0\rangle\big|_{\,\lambda=y}\,, \tag{16}$$

$$\langle \boldsymbol{f}|V_{i\lambda}|\boldsymbol{f}'\rangle = \frac{4\pi}{(\boldsymbol{f}-\boldsymbol{f}')^2+\lambda^2}\,. \tag{17}$$

In Eq. (16), after taking the derivative with respect to λ, one should set $\lambda = y$ and then perform the contour integration enclosing the pole at $y = \eta_n$ in the positive direction. In coordinate space, an integral representation similar to formula (16) was suggested in work [2].

Taking into account Eqs. (15) and (16), the integration over the intermediate momentum $\boldsymbol{f}_2$ in the amplitude (3) yields

$$\int\frac{d\boldsymbol{f}_2}{(2\pi)^3}\langle\psi_{ns}|\boldsymbol{f}_2\rangle\langle\boldsymbol{f}_2-\boldsymbol{f}|\psi_{1s}\rangle = N_1N_n(2\eta)^{-1}\oint\limits_{(\eta_n^+)}\frac{dy}{2\pi i}\frac{(y+\eta_n)^n}{(y-\eta_n)^n}\Big(-\frac{\partial}{\partial\lambda}\Big)\langle \boldsymbol{f}|V_{i\lambda}|0\rangle\big|_{\,\lambda=\eta+y}\,, \tag{18}$$

after the closure relation for the complete system of plane waves

$$\int\frac{d\boldsymbol{f}}{(2\pi)^3}|\boldsymbol{f}\rangle\langle\boldsymbol{f}| = 1 \tag{19}$$

has been used.

The Coulomb functions of the continuous spectrum can be represented as follows [13]

$$\langle \boldsymbol{f}|\psi_p\rangle = N_p\hat{\mathcal{I}}_\xi(t)\Big(-\frac{\partial}{\partial\varepsilon}\Big)\langle \boldsymbol{f}|V_{pt+i\varepsilon}|\boldsymbol{p}(1-t)\rangle\big|_{\varepsilon\to 0}\,, \tag{20}$$

$$\hat{\mathcal{I}}_\xi(t) = \frac{1}{2\pi i}\oint_\gamma\frac{dt}{t}\Big(\frac{-t}{1-t}\Big)^{i\xi}\,,\quad N_p^2 = \frac{2\pi\xi}{1-e^{-2\pi\xi}}\,, \tag{21}$$

where $\xi = \eta/p$. The integration contour γ in the integral operator $\hat{\mathcal{I}}_\xi(t)$ is a closed curve enclosing the points 0 and 1 once anti-clockwise. After taking the derivative in Eq. (20), the parameter ε should be tend to zero.

The integrations over $\boldsymbol{f}$ and $\boldsymbol{f}_1$ in the amplitude (3) can be evaluated by using Eq. (19) and the identity

$$f^{-2}\langle \boldsymbol{f}|V_{i\lambda}|0\rangle = \lambda^{-2}\langle \boldsymbol{f}|(V_0 - V_{i\lambda})|0\rangle\,. \tag{22}$$

The contour integrations arising from the functions ψ_{ns} and ψ_{p_1} are performed according to the theorem about residues. Then one obtains

$$\mathcal{A}_a = (4\pi)^2\alpha N_1N_nN_pN_{p_1}D_\lambda\frac{\partial}{\partial\lambda}\frac{\Phi(\lambda)}{\lambda^2}\big|_{\,\lambda=\eta+\eta_n}\,, \tag{23}$$

$$\Phi(\lambda) = \hat{\mathcal{I}}_\xi(t)\frac{[(\boldsymbol{p}_1-\boldsymbol{p}(1-t))^2-(pt+i\lambda)^2]^{i\xi_1-1}}{[p^2(1-t)^2-(p_1+pt+i\lambda)^2]^{i\xi_1}}\,, \tag{24}$$

$$D_\lambda = \sum_{k=0}^{n-1}\frac{(n-1)!(2\eta_n)^k}{(n-k-1)!k!(k+1)!}\frac{\partial^k}{\partial\lambda^k}\,,\quad N_{p_1}^2 = \frac{2\pi\xi_1}{1-e^{-2\pi\xi_1}}\,, \tag{25}$$

where $\xi_1 = \eta/p_1$, $N_1^2 = \eta^3/\pi$, and $N_n^2 = \eta_n^3/\pi$. After taking the derivatives with respect to λ, one should set $\lambda = \eta+\eta_n$. The contour integration in Eq. (24) is reduced to the hypergeometric function [14, 15]

$$\Phi(\lambda) = \frac{[\lambda^2+(\boldsymbol{p}-\boldsymbol{p}_1)^2]^{i\xi+i\xi_1-1}}{[(\lambda-ip)^2+p_1^2]^{i\xi}[(\lambda-ip_1)^2+p^2]^{i\xi_1}}\,{}_2F_1(i\xi,i\xi_1,1,x)\,, \tag{26}$$

$$x = \frac{2[(\boldsymbol{p}\cdot\boldsymbol{p}_1)-pp_1]}{\lambda^2+(p-p_1)^2}\,. \tag{27}$$

Since the exchange amplitude (4) is evaluated in the similar manner, we shall present here its explicit expression only. In the following, it is convenient to introduce the dimensionless amplitudes $\mathcal{M}_i$, $(i = a, b)$, which are related with amplitudes (3) and (4) via

$$\mathcal{A}_i = (4\pi)^2 \alpha N_1 N_n N_p N_{p_1} \eta^{-5} \mathcal{M}_i \,. \tag{28}$$

In $\mathcal{M}_i$, all momenta are expressed in units of $\eta = m\alpha Z$, while the energies are measured in units of $I = \eta^2/(2m)$. The dimensionless momenta of the incident and scattered electrons are given by $\boldsymbol{k} = \boldsymbol{p}/\eta$ and $\boldsymbol{k}_1 = \boldsymbol{p}_1/\eta$, respectively. The corresponding dimensionless energies $\varepsilon = k^2 = \xi^{-2}$ and $\varepsilon_1 = k_1^2 = \xi_1^{-2}$ are related with each other due to the energy-conservation law as $\varepsilon_1 = \varepsilon - \varepsilon_{\rm th}$, where $\varepsilon_{\rm th} = 1 - n^{-2}$.

The explicit expressions for the dimensionless amplitudes read

$$\mathcal{M}_a = D_\lambda \frac{\partial}{\partial\lambda} \frac{\Phi(\lambda)}{\lambda^2} \Big|_{\,\lambda=1+n^{-1}} \,, \tag{29}$$

$$\Phi(\lambda) = \frac{[\lambda^2 + (\boldsymbol{k} - \boldsymbol{k}_1)^2]^{i\xi + i\xi_1 - 1}}{[(\lambda - ik)^2 + k_1^2]^{i\xi} [(\lambda - ik_1)^2 + k^2]^{i\xi_1}} \, {}_2F_1(i\xi, i\xi_1, 1, x) \,, \tag{30}$$

$$x = \frac{2[(\boldsymbol{k}\cdot\boldsymbol{k}_1) - kk_1]}{\lambda^2 + (k - k_1)^2} \,, \tag{31}$$

$$D_\lambda = \sum_{l=0}^{n-1} \frac{(n-1)!}{(n-l-1)!l!(l+1)!} \Big(\frac{2}{n}\Big)^l \frac{\partial^l}{\partial\lambda^l} \,, \tag{32}$$

$$k = \sqrt{\varepsilon} = \xi^{-1} \,, \quad k_1 = \sqrt{\varepsilon_1} = \sqrt{\varepsilon - \varepsilon_{\rm th}} = \xi_1^{-1} \,, \tag{33}$$

$$\mathcal{M}_b = iD_\lambda \frac{\partial^2}{\partial\lambda\partial\nu} \hat{\mathcal{I}}_\xi(t) \int\limits_0^1 \frac{dy}{A\Lambda} \Big(\frac{A}{B}\Big)^{i\xi_1} \Big|_{\nu=1}^{\lambda=n^{-1}} \,, \tag{34}$$

$$A = [\boldsymbol{k}(1-t)y^2 - \boldsymbol{k}_1]^2 - (y\Lambda + i\nu)^2 \,, \tag{35}$$

$$B = k^2(1-t)^2 y^4 - (k_1 + y\Lambda + i\nu)^2 \,, \tag{36}$$

$$\Lambda = \sqrt{(kt + i\lambda)^2 - k^2(1-t)^2(1-y^2)} \,. \tag{37}$$

The differential cross section for the $1s \to ns$ excitation is related to the amplitude (2) via

$$d\sigma^*_{ns} = \frac{2\pi}{v} \overline{|\mathcal{A}|^2} \frac{d\boldsymbol{p}_1}{(2\pi)^3} \, \delta(E_p - E_{p_1} + E_{1s} - E_{ns}) \,, \tag{38}$$

$$\mathcal{A} = (4\pi)^2 \alpha N_1 N_n N_p N_{p_1} \eta^{-5} (\mathcal{M}_a \, \delta_{\tau_1'\tau_1} \delta_{\tau_2'\tau_2} - \mathcal{M}_b \, \delta_{\tau_2'\tau_1} \delta_{\tau_1'\tau_2}) \,. \tag{39}$$

Here $v = p/m$ is the absolute value of velocity of the incident electron. The line over $|\mathcal{A}|^2$ implies averaging over the polarizations of the initial electrons and summation over the polarizations of the final electrons. This can be done by the following relation

$$\overline{|\mathcal{A}|^2} = \frac{1}{4} \sum_{\tau_1,\tau_1'} \sum_{\tau_2,\tau_2'} |\mathcal{A}|^2 \,, \tag{40}$$

where summations are performed over the electron polarizations in both the initial and final states. The phase-space volume element for electrons scattered into the solid angle $d\Omega_1$ can be written as

$$d\boldsymbol{p}_1 = mp_1 \, dE_1 \, d\Omega_1 = 2\pi m p_1 \, dE_1 \, \sin\theta d\theta \,, \tag{41}$$

where θ is the angle between the vectors $\boldsymbol{p}$ and $\boldsymbol{p}_1$.

Performing integration over the energy yields the angular distribution of the scattered electrons

$$\frac{d\sigma^*_{ns}}{d\Omega_1} = \frac{\sigma_0}{Z^4} \, F_n(\varepsilon, \theta) \,, \tag{42}$$

$$F_n(\varepsilon, \theta) = \frac{2^8\pi}{n^3\varepsilon} \frac{|\mathcal{M}|^2}{(1 - e^{-2\pi\xi})(1 - e^{-2\pi\xi_1})} \,, \tag{43}$$

$$|\mathcal{M}|^2 = \frac{1}{4}|\mathcal{M}_+|^2 + \frac{3}{4}|\mathcal{M}_-|^2 \,, \tag{44}$$

where $\sigma_0 = \pi a_0^2$, $a_0 = 1/(m\alpha)$, and $\mathcal{M}_\pm = \mathcal{M}_a \pm \mathcal{M}_b$.

The total cross section reads

$$\sigma_{ns}^* = \frac{\sigma_0}{Z^4} Q_n(\varepsilon)\,, \tag{45}$$

$$Q_n(\varepsilon) = 2\pi \int_0^\pi F_n(\varepsilon,\theta)\sin\theta d\theta\,. \tag{46}$$

The functions (43) and (46) do not depend on the nuclear charge Z. In contrast with the Born approximation, Eqs. (42)–(46) are valid for arbitrary non-relativistic energies characterized by $\varepsilon_{\text{th}} \leqslant \varepsilon \ll 2(\alpha Z)^{-2}$.

In Fig. 2, the universal function (43) is calculated for the principal quantum number $n = 2$ within the near-threshold energy domain. For $\varepsilon_{\text{th}} \leqslant \varepsilon \lesssim 2\varepsilon_{\text{th}}$, the electron backward scattering is more preferable than the forward scattering. With increasing energy ε, the electrons are scattered predominantly in the forward direction ($\theta \lesssim \pi/4$). For small values $n \gtrsim 2$, the dependence of $n^3 F_n(\varepsilon,\theta)$ on n is rather weak. With increasing n, the curves $n^3 F_n(\varepsilon,\theta)$ tend to the unique limiting surface.

In Fig. 3, the universal functions (46) are calculated for several values of n. Although the Born approximation is formally legitimate only in the high-energy range $1 \ll \varepsilon \ll 2(\alpha Z)^{-2}$, it turns out to be in a fair agreement with exact results also within the near-threshold domain. The limiting values of the functions (46) at the threshold points $\varepsilon = \varepsilon_{\text{th}}$ are given in Table I.

In the case of helium-like multicharged ions, the inelastic electron scattering followed by the excitation of a K-shell electron into the $2s$ state is considered in work [16]. For targets characterized by the small parameters $1/Z$ and αZ, our calculations performed within the framework of the non-relativistic perturbation theory are in good agreement with those obtained by the relativistic distorted-wave method [17]. For example, according to K.L. Wong *et al* [17], the cross sections for near-threshold excitation of the forbidden line z ($1s2s\,^3S_1 \to 1s^2\,^1S_0$) in helium-like ions Ti, V, Cr, Mn, and Fe are known to be 118 b, 101 b, 85 b, 73 b, and 64 b, respectively. These values should be compared with our predictions, which are equal to 117 b, 98 b, 82 b, 70 b, and 60 b, respectively.

III. POSITRON IMPACT

As in the case of the electron impact, the incident positron can be characterized by the energy $E_p = \boldsymbol{p}^2/(2m)$ and the asymptotic momentum $\boldsymbol{p}$, while the scattered positron is characterized by the energy $E_{p_1} = \boldsymbol{p}_1^2/(2m)$ and the asymptotic momentum $\boldsymbol{p}_1$. The energy-conservation law keeps the same form, namely, $E_p + E_{1s} = E_{p_1} + E_{ns}$. Since the interacting particles are not identical, the exchange effect is absent. Accordingly, the ionization process is represented merely by the diagram depicted in Fig. $1(a)$. The transition to the dimensionless quantities can be performed in the same manner as in the case of the electron impact. The formulas (29)–(33) hold true with the only exception that in Eq. (30) one has to make the following substitutions: $\xi \to -\xi$ and $\xi_1 \to -\xi_1$. The differential cross section, which describes the universal angular distributions for scattered positrons, is given by Eqs. (42) and (43), where $\mathcal{M} = \mathcal{M}_a$.

In Fig. 4, the universal function (43) is calculated for $n = 2$ within the near-threshold energy domain $\varepsilon_{\text{th}} \leqslant \varepsilon \leqslant 7.5$. The characteristic behaviour of $n^3 F_n(\varepsilon,\theta)$ with respect to the variables ε and θ remains similar also for other values of the principal quantum number n. The positron scattering occurs preferably in the forward cone ($\theta \lesssim \pi/4$), while backward scattering is suppressed. The dominant contribution to the total cross section arises from the small angles θ close to zero.

In Fig. 5, the universal functions (46) are calculated for a few values of n. As can be seen, the functions $n^3 Q_n(\varepsilon)$ are quickly degenerated into the unique curve with increasing n. For the energies $\varepsilon \sim \varepsilon_{\text{th}}$, the cross sections are strongly suppressed. Since the high-energy Born asymptotes do not depend on the signature of charge of the projectiles, Eqs. (9)–(12) are applicable for the positron scattering in the energy range $1 \ll \varepsilon \ll 2(\alpha Z)^{-2}$.

IV. ANTIPROTON IMPACT

In comparison with the electron, the antiproton has the same electric charge, but much larger mass $M \gg m$. We shall use the notations $E_p = \boldsymbol{p}^2/(2M)$ and $\boldsymbol{p} = Mv$ for the energy and asymptotic momentum of the projectile, respectively. The scattered antiproton is characterized by the energy $E_{p_1} = \boldsymbol{p}_1^2/(2M)$ and the asymptotic momentum $\boldsymbol{p}_1$. Then the energy-conservation law reads as usual: $E_p + E_{1s} = E_{p_1} + E_{ns}$. However, now it is convenient to express the energies of the incident and scattered particles by the characteristic binding energy $\tilde{I} = M(\alpha Z)^2/2$, namely, $\varepsilon = E_p/\tilde{I}$ and $\varepsilon_1 = E_{p_1}/\tilde{I}$. In this case, the dimensionless energy $\varepsilon = v^2/(\alpha Z)^2$ does not depend on the mass of the incident particle. The energy-conservation law for the dimensionless quantities is given by $\varepsilon = \varepsilon_1 + \varepsilon_{\text{th}}$, where $\varepsilon_{\text{th}} = \mu(1 - n^{-2})$ is the threshold energy and $\mu = m/M$ is the mass ratio.

In the near-threshold energy domain $\varepsilon \gtrsim \varepsilon_{\text{th}}$, the antiproton momenta can be estimated as follows $p \sim p_1 \sim \eta/\sqrt{\mu} \gg \eta$. Due to significant difference in masses ($\mu \simeq 1/1836.15$), the momentum of the antiproton is much larger than the average momentum of the K-shell electron. However, the velocity of the antiproton is much smaller than the characteristic velocity of the bound

electron: $v \sim \alpha Z\sqrt{\mu} \ll \alpha Z$. This situation corresponds to the quasi-classical regime [18]. However, we describe it within the framework of the consistent quantum approach.

Since the interacting particles are not identical, the exchange effect is absent and $\mathcal{M} = \mathcal{M}_a$. The formulas (29)–(32) apply analogously for the case of the antiproton impact. However, the dimensionless variables should be understood now as follows

$$\xi = \frac{1}{k\mu} = \frac{1}{\sqrt{\varepsilon}}\,, \quad \xi_1 = \frac{1}{k_1\mu} = \frac{1}{\sqrt{\varepsilon_1}} = \frac{1}{\sqrt{\varepsilon - \varepsilon_{\rm th}}}\,, \quad \varepsilon_{\rm th} = \mu(1 - n^{-2})\,. \tag{47}$$

The angular distribution of the scattered antiprotons is given by Eq. (42), but the function $F_n(\varepsilon, \theta)$ now reads

$$F_n(\varepsilon, \theta) = \frac{2^8\pi}{n^3\varepsilon} \frac{\mu^{-2}|\mathcal{M}|^2}{(1 - e^{-2\pi\xi})(1 - e^{-2\pi\xi_1})}\,. \tag{48}$$

The total cross section σ^*_{ns} is again reduced to Eqs. (45) and (46).

For very slow collisions ($\varepsilon \sim \varepsilon_{\rm th}$), the functions (48) exhibit the well-pronounced maximum in the backward scattering ($\theta \simeq \pi$) (see Fig. 6). For energies $\varepsilon \gtrsim 10\varepsilon_{\rm th}$, the antiprotons are scattered predominantly at small angles ($0 < \theta \lesssim \pi/4$). With increasing the incident energies, the domain of the scattering angles, at which the excitation cross section is exhausted, narrows. The scattering at the angle $\theta = 0$ becomes significant for $\varepsilon \gtrsim 150\varepsilon_{\rm th}$, while it dominates for $\varepsilon \gtrsim 160\varepsilon_{\rm th}$.

In Fig. 7, the universal functions $n^3Q_n(\varepsilon)$ are calculated for a few values of n. The asymptotic high-energy range, where one can justify application of the Born approximation, is characterized by $1 \ll \varepsilon \ll 2(\alpha Z)^{-2}$. It is easy to check that the formulas (9)–(12) are also valid for the case of fast projectiles with the arbitrary mass, in particular, for antiproton impact. The exact functions (46) approach the high-energy limits (10), when $\varepsilon \gtrsim 10$. Near the threshold, the total cross section has the maximum, which originates from the backward scattering. The limiting values of the functions (46) at the threshold points $\varepsilon = \varepsilon_{\rm th}$ are calculated in Table I.

V. PROTON IMPACT

The proton has the same electric charge as positron and the same mass M as antiproton ($M \gg m$). In order to keep the usual expression for the energy-conservation law, we shall use the standard notations for the energies and asymptotic momenta of incident and scattered particles. As in the case of the antiproton impact, the energies are scaled by the characteristic binding energy $\tilde{I} = M(\alpha Z)^2/2$, namely, $\varepsilon = E_p/\tilde{I}$ and $\varepsilon_1 = E_{p_1}/\tilde{I}$. The excitation process $1s \to ns$ can occur due to impact of particle with the energy $\varepsilon \geqslant \varepsilon_{\rm th} = \mu(1 - n^{-2})$, where the mass ratio $\mu = m/M$. The formulas (29)–(32) can be used for the case of the proton impact, but in Eq. (30) one needs to make the following substitutions: $\xi \to -\xi$ and $\xi_1 \to -\xi_1$. The dimensionless variables ξ and ξ_1 are defined by Eq. (47). The angular distribution for scattered protons is given by Eqs. (42) and (48), together with $\mathcal{M} = \mathcal{M}_a$.

For the low-energy collisions ($\varepsilon \sim \varepsilon_{\rm th}$), the functions (48) are strongly suppressed. For energies $\varepsilon \gg \varepsilon_{\rm th}$, the angular distributions for the proton impact have similar behaviour as those for the antiproton impact (compare Figs. 8 and 6). In Fig. 9, the universal functions $n^3Q_n(\varepsilon)$ are calculated exactly (according to Eqs. (46) and (48)) and within the Born approximation (according to Eqs. (10)–(12)). The latter is applicable for the asymptotically high energies characterized by $1 \ll \varepsilon \ll 2(\alpha Z)^{-2}$.

VI. CONCLUSIONS

We have investigated the excitation process $1s \to ns$ of hydrogen-like multicharged ions by impact of different charged particles, such as electrons, positrons, protons, and antiprotons. The atomic targets are assumed to be characterized by small parameters $1/Z$ and αZ. The universal scaling behaviour for the differential and total cross sections is deduced within the framework of the perturbation theory, taking into account the one-photon exchange diagrams. The results obtained are valid for the non-relativistic energies, including the near-threshold energy domain.

Acknowledgments

The authors acknowledge financial support from GSI Helmholtz Center for Heavy Ion Research. AVN is grateful to the Dresden University of Technology for hospitality and for financial support from Max Planck Institute for the Physics of Complex Systems.

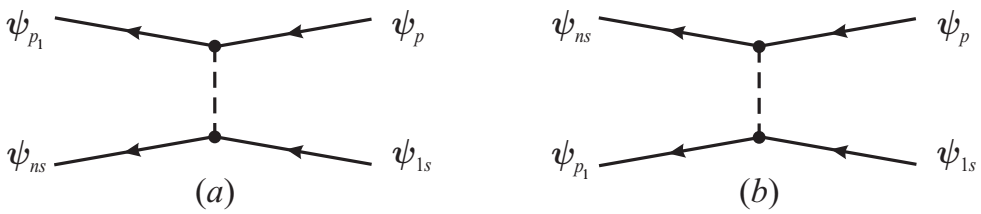

FIG. 1: Feynman diagrams for excitation of the K-shell electron by electron impact. Solid lines denote electrons in the external Coulomb field of the nucleus, while dashed line denotes the electron-electron Coulomb interaction.

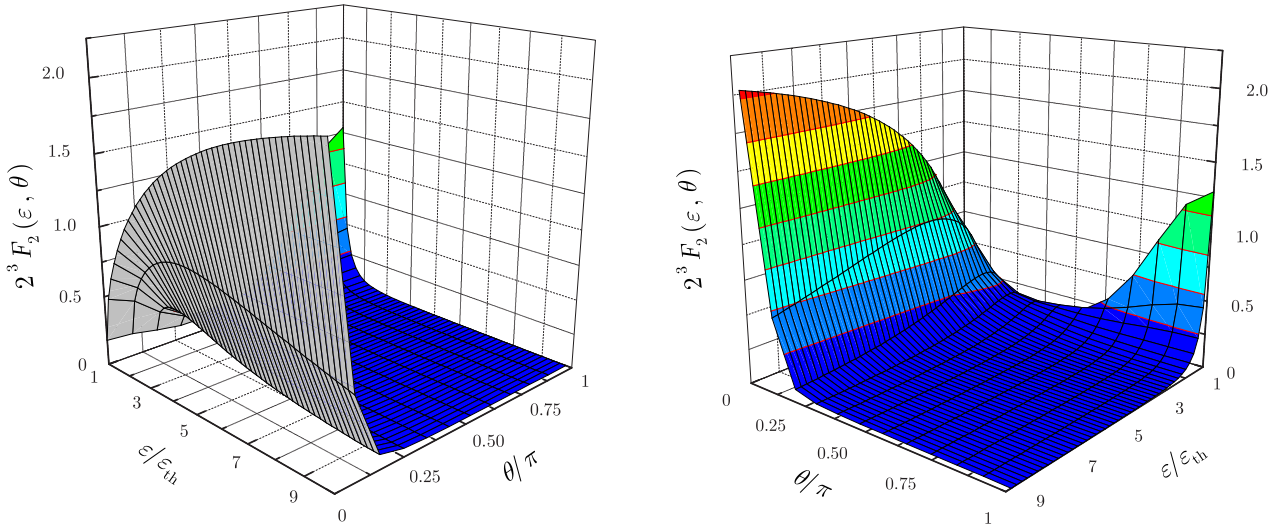

FIG. 2: The universal function (43) is calculated for $n = 2$. The variable ε is the energy of incident electron, which is scattered at the angle θ with respect to direction of the initial momentum $\boldsymbol{p}$. (Colour online.)

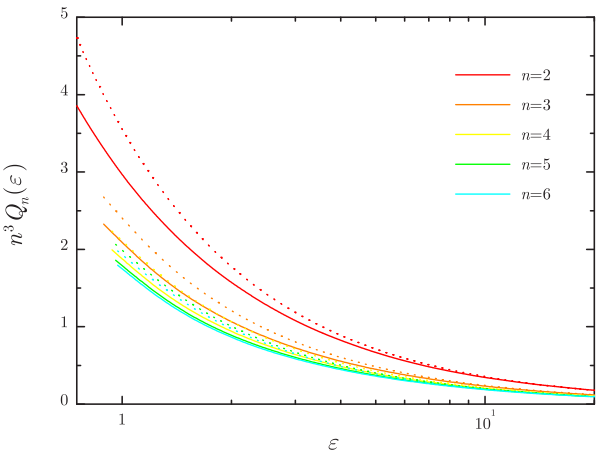

FIG. 3: The universal functions $n^3 Q_n(\varepsilon)$ for the case of the electron impact. The solid lines are the exact calculations, dashed lines are the Born approximations. (Colour online.)

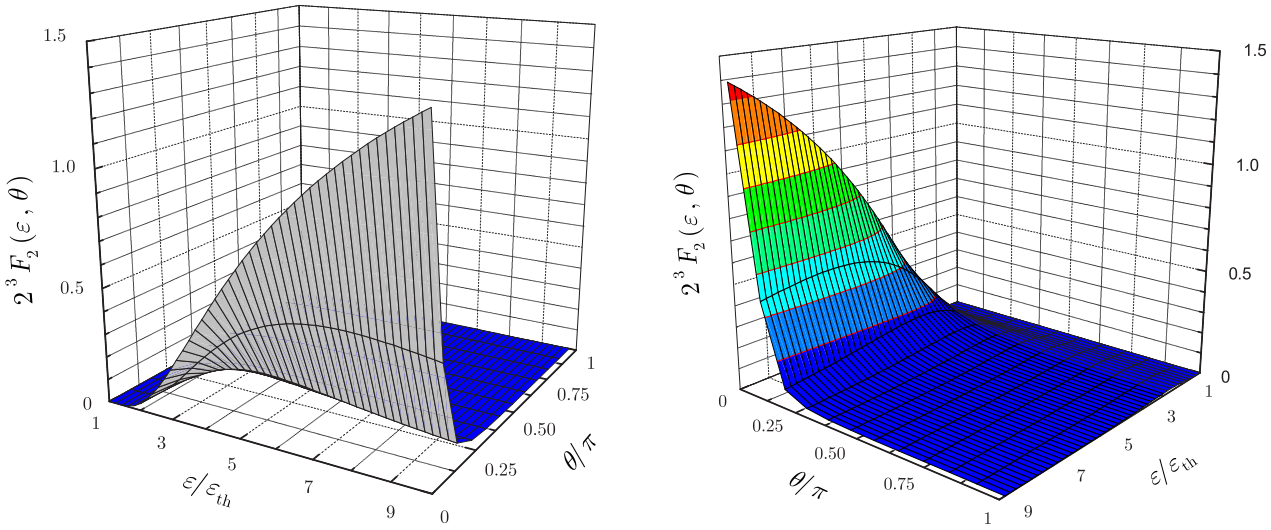

FIG. 4: The universal function (43) is calculated for $n = 2$. The variable ε is the energy of incident positron, which is scattered at the angle θ. (Colour online.)

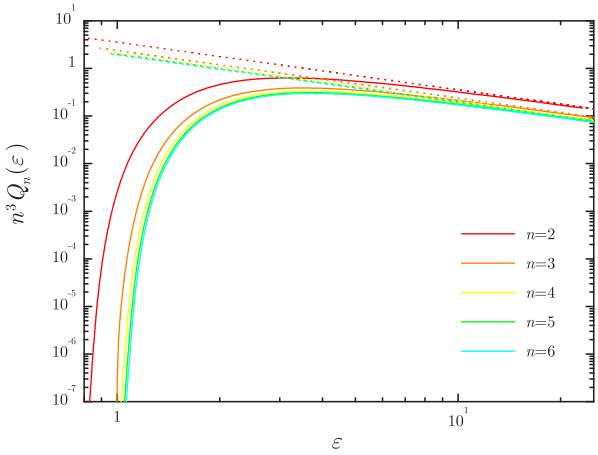

FIG. 5: The universal functions $n^3 Q_n(\varepsilon)$ for the case of the positron impact. The solid lines are the exact calculations, dashed lines are the Born approximations. (Colour online.)

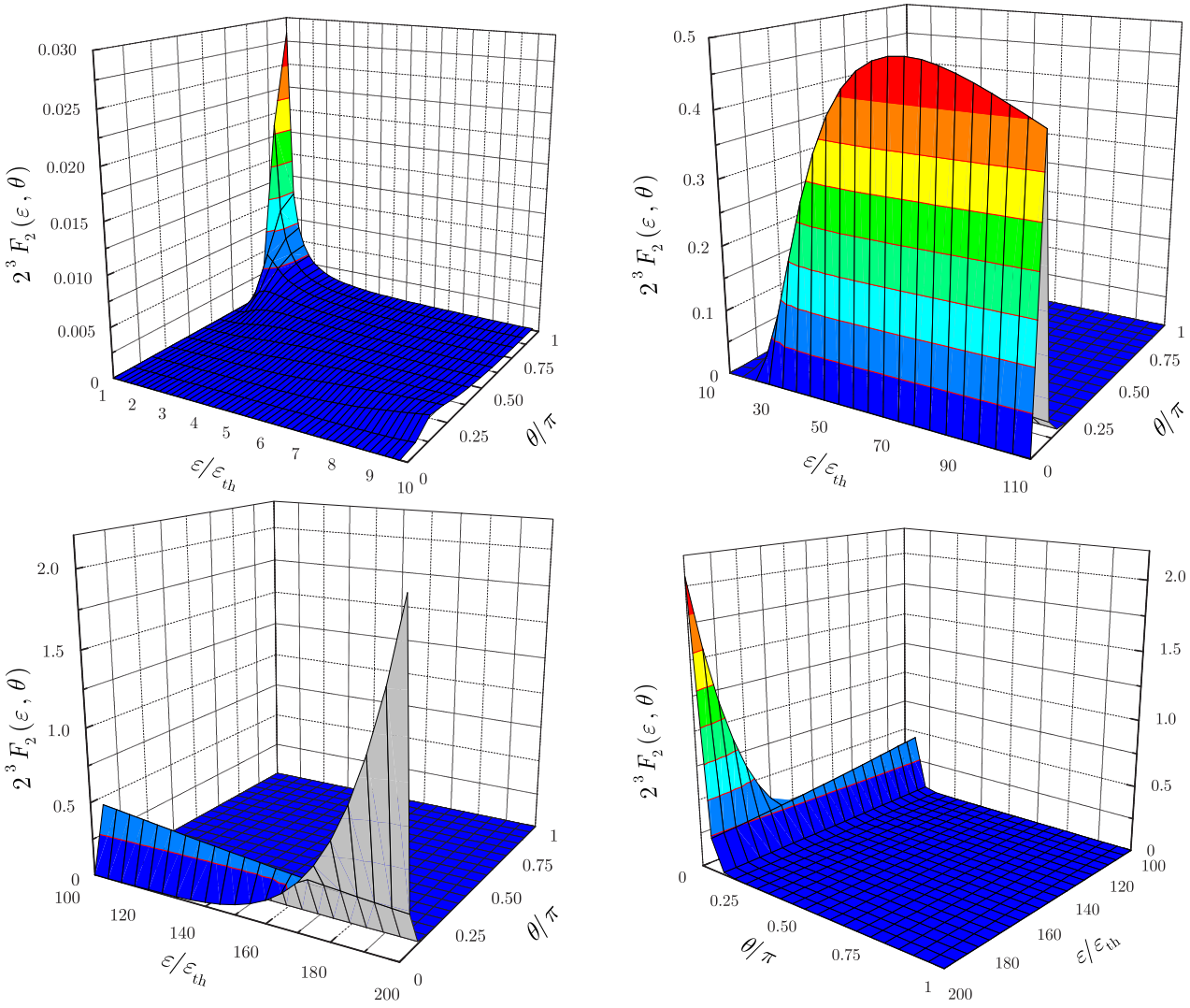

FIG. 6: The universal function (48) is calculated for $n = 2$ in the case of the antiproton impact. (Colour online.)

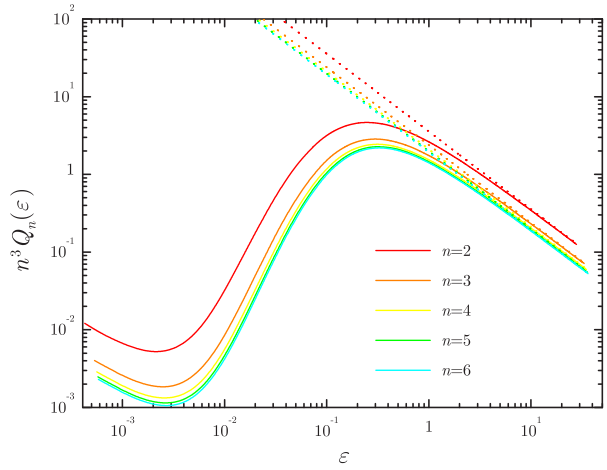

FIG. 7: The universal functions $n^3 Q_n(\varepsilon)$ for the case of the antiproton impact. The solid lines are the exact calculations, dashed lines are the Born approximations. (Colour online.)

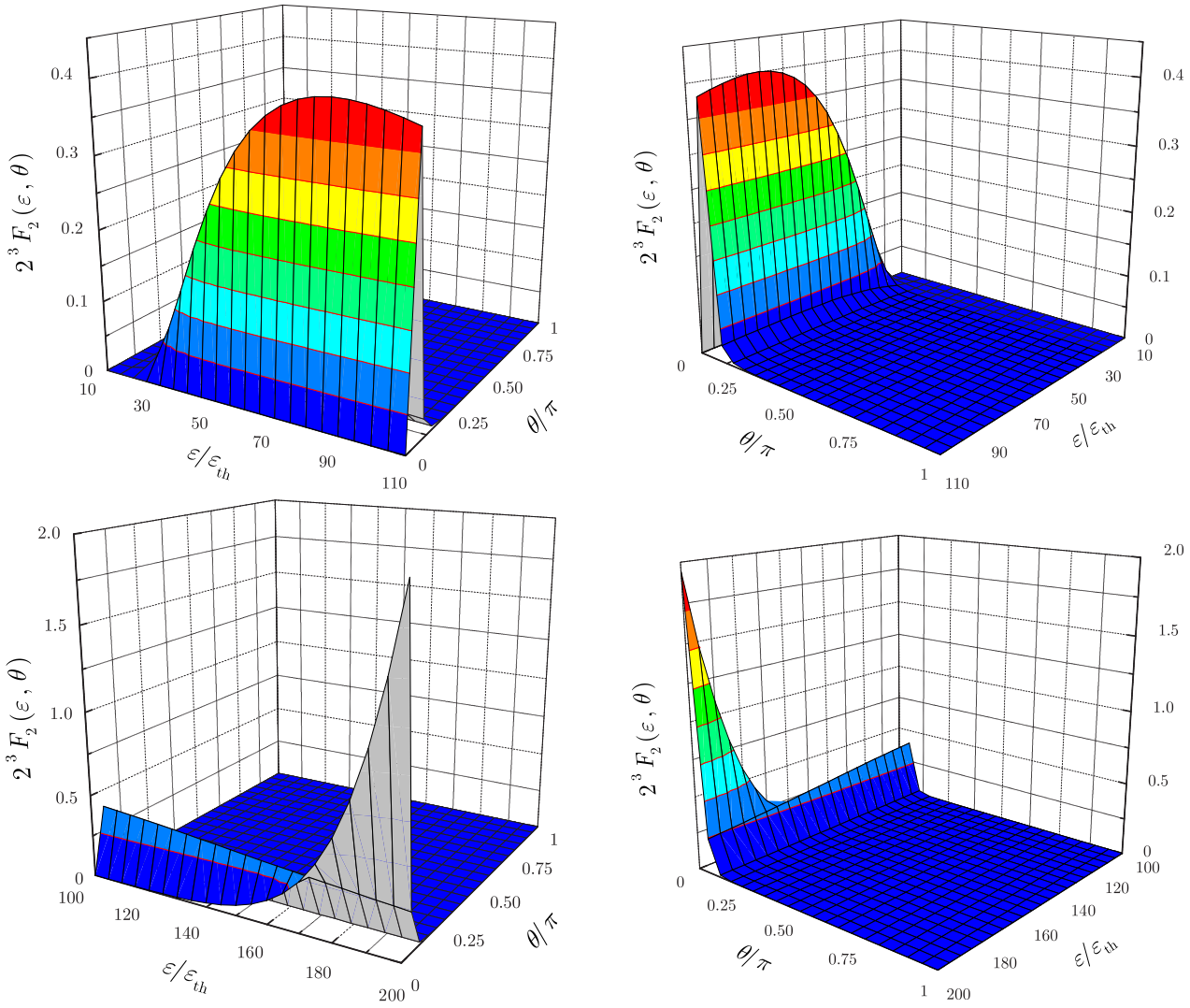

FIG. 8: The universal function (48) is calculated for $n = 2$ in the case of the proton impact. (Colour online.)

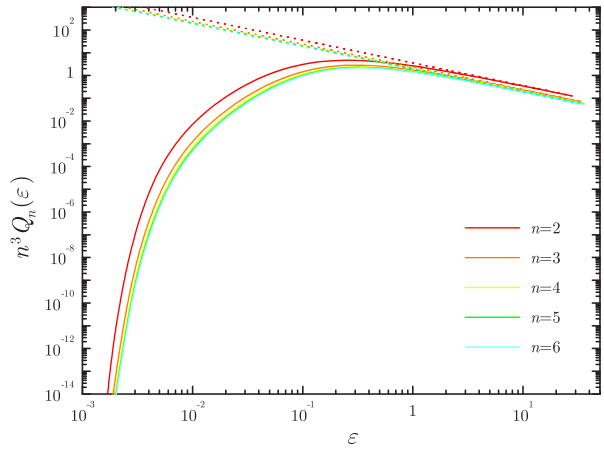

FIG. 9: The universal functions $n^3 Q_n(\varepsilon)$ for the case of the proton impact. The solid lines are the exact calculations, dashed lines are the Born approximations. (Colour online.)

TABLE I: For various principal quantum numbers n, the numerical coefficients (12), the threshold energies $\varepsilon_{\rm th}$ for electron (positron) and (anti)proton impact, and the threshold values of the functions (46) for the electron and antiproton impact are tabulated.

n	$\varkappa_n$	$\varepsilon_{\rm th}=\mu(1-n^{-2})$		$n^3Q_n(\varepsilon_{\rm th})$	
		$\mu=1$	$\mu=1/1836.15$	electron	antiproton
2	3.5515	$3/4$	$0.40846\cdot10^{-3}$	3.855	0.01256
3	2.3798	$8/9$	$0.48410\cdot10^{-3}$	2.326	0.00430
4	2.0971	$15/16$	$0.51058\cdot10^{-3}$	1.992	0.00308
5	1.9819	$24/25$	$0.52283\cdot10^{-3}$	1.860	0.00267
6	1.9230	$35/36$	$0.52949\cdot10^{-3}$	1.794	0.00245

[1] M. Inokuti, Rev. Mod. Phys. 43 (1971) 297.
[2] C. Sinha, N. Roy and N.C. Sil, J. Phys. B 11 (1978) 1807.
[3] J.E. Potter and J. Macek, Phys. Rev. A 20 (1979) 2302.
[4] R.J.W. Henry, Phys. Rep. 68 (1981) 1.
[5] S. Saxena, G.P. Gupta and K.C. Mathur, J. Phys. B 17 (1984) 3743.
[6] Y. Itikawa, Phys. Rep. 143 (1986) 69.
[7] Y. Itikawa, Atomic Data Nucl. Data Tables 63 (1996) 315.
[8] P.S. Krstić, D.R. Schultz and R.K. Janev, J. Phys. B 29 (1996) 1941.
[9] K. Sakimoto, J. Phys. B 33 (2000) 5165.
[10] A. Ghoshal and P. Mandal, Phys. Rev. A 72 (2005) 032714.
[11] E.J. Kelsey, Ann. Phys. 322 (2007) 1925.
[12] A.V. Nefiodov and G. Plunien, Phys. Lett. A 372 (2008) 1645.
[13] V.G. Gorshkov, A.I. Mikhailov and V.S. Polikanov, Nucl. Phys. 55 (1964) 273.
[14] A. Nordsieck, Phys. Rev. 93 (1954) 785.
[15] S.D. Oh, J. Macek and E. Kelsey, Phys. Rev. A 17 (1978) 873.
[16] A.V. Nefiodov and G. Plunien, Phys. Lett. A 371 (2007) 432.
[17] K.L. Wong, P. Beiersdorfer, K.J. Reed and D.A. Vogel, Phys. Rev. A 51 (1995) 1214.
[18] L.D. Landau and E.M. Lifshitz 1991 Quantum Mechanics: Non-relativistic Theory (Oxford: Pergamon)